Geomechanics and Engineering, *Vol. 31, No. 4 (2022) 423-437*
https://doi.org/10.12989/gae.2022.31.4.423

Prediction of dynamic behavior of full-scale slope based on the reduced scale 1 g shaking table test

Yong Jin[1a], Daehyeon Kim*[1], Sugeun Jeong[1b] and Kyungho Park[2c]

[1]*Department of Civil Engineering, Chosun University, 309 Pilmun-daero, Dong-gu, Gwangju, Republic of Korea*
[2]*Department of Civil Construction Engineering, Chosun College of Science and Technology, 309-1 Pilmun-daero, Dong-gu, Gwangju, Republic of Korea*

(*Received May 4, 2022, Revised November 9, 2022, Accepted November 22, 2022*)

Abstract. The objective of the study is to evaluate the feasibility of the dynamic behavior of slope through both 1 g shaking table test and numerical analysis. Accelerometers were installed in the slope model with different types of seismic waves. The numerical analysis (ABAQUS and DEEPSOIL) was used to simulate 1 g shaking table test at infinite boundary. Similar Acceleration-time history, Spectral acceleration (SA) and Spectral acceleration amplification factor (Fa) were obtained, which verified the feasibility of modeling using ABAQUS and DEEPSOIL under the same size. The influence of the size (1, 2, 5, 10 and 20 times larger than that used in the 1 g shaking table test) of the model used in the numerical analysis were extensively investigated. According to the similitude law, ABAQUS was used to analyze the dynamic behavior of large-scale slope model. The 5% Damping Spectral acceleration (SA) and Spectral acceleration amplification factor (Fa) at the same proportional positions were compared. Based on the comparison of numerical analyses and 1 g shaking table tests, it was found that the 1 g shaking table test result can be utilized to predict the dynamic behavior of the real scale slope through numerical analysis.

Keywords: 1 g shaking table test; ABAQUS; amplification; dynamic behavior of soil; infinite boundary; similarity law; slope

1. Introduction

1.1 Background

Landslides caused by earthquakes are one of the most dangerous geological hazards (Corominas *et al.* 2014). A landslide disaster is triggered when the magnitude of an earthquake is greater than 4.0. A large earthquake can induce tens of thousands of landslides with a distribution area of up to 500,000 square kilometers (Keefer 1984). During the Chi-Chi Earthquake (M_w 7.3) on September 21, 1999, 9272 landslides with an area of more than 625 square meters occurred (Liao and Lee 2000). The 2008 Wenchuan Earthquake (M_w 7.9) in China occurred in an area of 110,000 square kilometers with a total area of 1,160 square kilometers and 197,481 landslides (Xu *et al*. 2014). At least 22,914 landslides larger than 500 square meters occurred in Gorkha earthquake (M_w 7.8) Nepal in 2015 (Tian *et al*. 2020). The loss of life and property caused by earthquake.

Landslides can account for half or even more of the loss caused by the entire earthquake. Because of site constraints and the uncertainty of seismic occurrence, research on sites prone to seismic actions is very necessary. In order to better understand the characteristics of the site, it is necessary to study the dynamic behavior of the soil.

Shaking table test is an important means to study earthquake engineering problems. There are two most common types of shaking tables in the seismic field of geotechnical engineering. The 1 g shaking table test and the centrifuge test can simulate the dynamic behavior of a small-size model Due to the huge cost of centrifuge test equipment. Considering the economy of equipment operation, the 1 g shaking table has been more widely used in the laboratory. The 1 g shaking table test has the limitation that it cannot simulate the geostatic stress of the prototype soil. Therefore, it is necessary to use the simulation analysis to study the large-scale model according to the similarity law and the results of the 1 g shaking table test.

1.2 Previous studies

Similarity law is a branch of engineering science concerned with establishing the necessary and sufficient conditions of similarity among phenomena (Coutinho *et al.* 2016). By applying the law of proportionality to experimental results of a scale model related to a prototype through similarity conditions, engineers and scientists can accurately predict the behavior of a prototype, as shown in Fig. 1.

Scale model similarity describes the relationship between model and prototype behavior, which is the basis of determining the scale relationship. Rocha (1957) first systematically described the scale modeling of soil

*Corresponding author, Professor
E-mail: dkimgeo@chosun.ac.kr
[a]Ph.D.
[b]Ph.D.
[c]Professor

ISSN: 2005-307X (Print), 2092-6219 (Online)

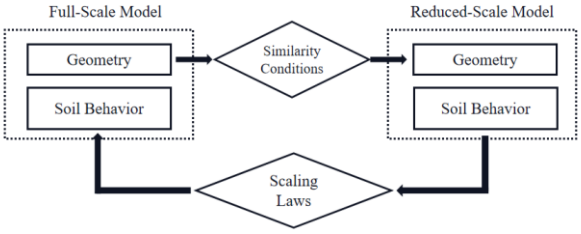

Fig. 1 Sketch for the prediction of the soil behavior of an oversized prototype

Table 1 Main similarity law of Iai

Items	Scaling Factor (prototype/ model)	Type 1 (λ_p=1)	Type 2 (λ_ε=$\lambda^{0.5}$, λ_p=1)	Type 3 (λ_ε=1, λ_p=1)
Length	λ	λ	λ	λ
Density	λ_p	1	1	1
Strain of soil	λ_ε	λ_ε	$\lambda^{0.5}$	1
Time	$(\lambda\lambda_\varepsilon)^{0.5}$	$(\lambda\lambda_\varepsilon)^{0.5}$	$\lambda^{0.75}$	$\lambda^{0.5}$
Total stress	$\lambda\lambda_p$	λ	λ	λ
Effective stress	$\lambda\lambda_p$	λ	λ	λ
Tangent modulus	$\lambda\lambda_p/\lambda_\varepsilon$	$\lambda/\lambda_\varepsilon$	$\lambda^{0.5}$	λ
Bulk modulus	$\lambda\lambda_p/\lambda_\varepsilon$	$\lambda/\lambda_\varepsilon$	$\lambda^{0.5}$	λ
Pressure	$\lambda\lambda_p$	λ	λ	λ
Permeability	$\lambda\lambda_p/\lambda_\varepsilon$	$\lambda/\lambda_\varepsilon$	$\lambda^{0.5}$	λ
Displacement	$\lambda\lambda_\varepsilon$	$\lambda\lambda_\varepsilon$	$\lambda^{1.5}$	λ
Velocity	$(\lambda\lambda_\varepsilon)^{0.5}$	$(\lambda\lambda_\varepsilon)^{0.5}$	$\lambda^{0.75}$	$\lambda^{0.5}$
Acceleration	1	1	1	1
Pore water flow	$(\lambda\lambda_\varepsilon)^{0.5}$	$(\lambda\lambda_\varepsilon)^{0.5}$	$\lambda^{0.75}$	$\lambda^{0.5}$
Porosity of soil	1	1	1	1
Flexural rigidity	$\lambda^4\lambda_p/\lambda_\varepsilon$	$\lambda^4/\lambda_\varepsilon$	$\lambda^{3.5}$	λ^4
Longitudinal rigidity	$\lambda^2\lambda_p/\lambda_\varepsilon$	$\lambda^2/\lambda_\varepsilon$	$\lambda^{1.5}$	λ^2
Bending moment of the beam	$\lambda^3\lambda_\varepsilon$	λ^3	λ^3	λ^3
Inclination of the beam	λ_ε	λ_ε	$\lambda^{0.5}$	λ
Shear force of the beam	$\lambda^2\lambda_p$	λ^2	λ^2	λ^2
Axial force of the beam	$\lambda^2\lambda_p$	λ^2	λ^2	λ^2
Density of the beam	λ_p	1	1	1
Traction of the beam	$\lambda\lambda_p$	λ	λ	λ

mechanics problems. Roscoe (1968) studied the difficulty of scale models in replicating the prototype constitutive behavior of soils. Kagawa (1978) considered the effect on the prototype and the model of the ratio of force, established the model of the structure can be applied to soil vibration experiment of similar rules. Iai (1989) derived the fundamental equations of similarity governing the equilibrium and mass balance of soil skeleton, pore water, pile and sheet pile structures, and external water. Meymand (1998) considered the similarity law derived by Iai and applied it to the behavior simulation of seismic piles in saturated clay. Turan *et al*. (2009) adopted a series of scale model tests and calculated the scale relationship between the prototype and the model according to the references.

Table 2 The law of similarity used in this study

Mass density	1	Acceleration	1	Length	λ
Frequency	λ^{-1}	Shear wave velocity	$\lambda^{-0.5}$	Stress	λ
Modulus	1	Time	$\lambda^{0.75}$	Strain	1

λ is the similarity ratio of the large-scale model to the laboratory size model

Sukkarak *et al.* (2018) developed a prediction method for considering the proportional effect of rockfill materials in the numerical deformation analysis of rockfill dam using 3D finite element analysis, which can consider the scale effect in the deformation analysis of the dam. Yang *et al*. (2018) studied the dynamic response and failure characteristics of anti-dip rock slope through a large-scale shaking table test. Seo *et al.* (2021) conducted a series of scale model tests in order to evaluate the initial failure behavior and failure mode of the tunnel-type anchorage.

Different scale models have different scale factors. The model needs this similarity relationship to satisfy all parameters in the system. With the development of research, frequency has also been used as one of the research parameters. Lin and Wang (2006) used the shaking table test to study the initiation of slope failure. The scale factor λ used in the experiment is 20. Based on similarity requirements, the control factor used in model testing is frequency. Chen *et al*. (2019) conducted shaking table test to study the damage mechanism of subway structure in soft soil when it experiences strong ground motion. It was found that the seismic responses of structures and soils are more sensitive to input motions with richer low-frequency components.

1.3 The objective of the study

In order to evaluate the feasibility of the dynamic behavior of slope through 1g shaking table test and numerical analysis. The 1g shaking table test results of the same size were compared with ABAQUS and DEEPSOIL. Although the DEEPSOIL is only suitable for the analysis of semi-infinite flat space. However, for the flat part of the slope sample, it can be simply verified. The experiment results of the flat part were compared with the results of ABAQUS and DEEPSOIL, and the experimental results of the slope part was compared with the results of ABAQUS. The results were very consistent, which indicates the feasibility of using ABAQUS for large scale model modeling.

The experimental results of 1 g shaking table test were studied by using the similarity law, and the seismic ground of large slope model is modeled by ABAQUS using these data, so as to analyze the dynamic characteristics of soil in large slope. According to Table 1, this research falls into the Type 2 category, and the following parameters were selected as reference for this research in Table 2. In addition, an example of additional parameters is illustrated in Table 5 below. On the basis of Iai's similarity law, frequency parameters were added to scale simulation of the frequency of the model, and the dynamic behavior of simulation results was consistent with the actual results.

Combined with the above methods, this paper provides more rigorous analysis results.

2. Materials and methods

2.1 Soil properties

In this study, the soil sample of 1 g shaking table test was collected at a power plant construction site at Ulju-gun, in the Ulsan Metropolitan City area in Korea. In order to analyze the performance of geotechnical engineering indexes of the soil sample, specific gravity test, particle size analysis test and standard processing machine test were carried out. The soil sample used was homogeneous and the degree of compaction was 98.5%, resulting in negligible settlement caused by gravity in the experiment. Jin *et al.* (2021) described the process of calculating elastic modulus by using shear wave velocity in 1 g shaking table test. Here, the average shear wave velocity obtained by hammer tests is 73.58 m/s, and the elastic modulus calculated by Young's modulus formula is $2x10^7$ Pa. Table 3 summarizes the test results for basic physical properties of the soil used in the study.

2.2 Experimental equipment

2.2.1 1 g shaking table

The experimental equipment in this study is mainly composed of 1 g shaking table test equipment system, laminar shear box, data logger and accelerometers. Fig. 2 shows a schematic diagram of the 1 g shaking table test system. The dynamic characteristics of soil can be obtained by 1g shaking table test with this system.

The uniaxial shaking table is used to test the response of the structure and verify the seismic simulation. The equipment simulates a variety of ground motions, including the reproduction of recorded seismic timelines and solid liquefaction and vibration tests. The system is powered by an electronic servo control valve with a high-precision closed-loop PID controller and can be used for any type of waveform, as well as waveforms generated by MATLAB. The specifications of the shaking table are shown in the Table 4.

2.2.2 Laminar shear box

The laminar shear box consists of 12 aluminum frames that move independently horizontally. Each frame is capable of simulating the infinitely expanding ground boundary conditions of horizontal shear motion. The dimensions of the structure are 2000 mm (L) x 600 mm (W) x 600 mm (H), each frame is 45 mm thick, and the spacing between the frames is about 5 mm. The 1 g shaking table has a uniaxial vibration mode in the X-axis direction. Fig. 3 shows the Laminar shear box and soil sample set up in the box.

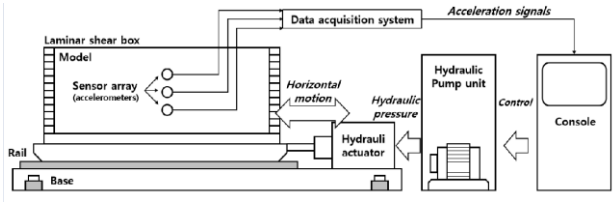

Fig. 2 The experimental system used in this study (Kim *et al.* 2020)

Table 3 Geotechnical index properties of the soil used in this study

Parameter	Value	Parameter	Value
No. 200 Passing (%)	10.8	e_{max}	1.123
G_s	2.69	e_{min}	0.443
OMC (%)	12.5	$r_{d\,max}$ (kN/m^3)	18.27
PI (%)	NP	$r_{d\,min}$ (kN/m^3)	12.43
USCS	SW-SM	Elastic modulus (Pa)	$2x10^7$
Internal friction angle (°)	27.7	Dilatancy angle (°)	24.4

Table 4 Uniaxial shaking table parameters and operating specifications

Item	Specification
Table size (mm)	2000×600
Maximum acceleration (g)	1
Full play load (kg)	1800
Table stroke (mm)	200(±100)
Payload capacity (kg)	5000
Operating frequency (Hz)	10

(a) Laminar shear box in this study

(b) Soil sample set up in the box

Fig. 3 Laminar shear box

2.2.3 Data logger and accelerometer

Data logging is the measuring and recording of physical or electrical parameters over a period of time. Accelerometers are used to capture seismic acceleration. ARF-20A acceleration transducer which can measure up to 20m/s², was used as the accelerometer for this study. The data logger used is the 24 channels SDL-350R model which is compatible with ARF-20A, and capable of data storage intervals up to 0.005 seconds. Fig. 4 shows the data logger and accelerometer used in this study.

At the midpoint of the model, accelerometer 1 to accelerometer 6 were set at vertical intervals of 10cm. In order to test the acceleration of the top, accelerometer 7 is placed only 5 cm beneath the top. Through our previous experiments, it has been shown that an accelerometer directly placed on the surface is not conducive to the capture of the top acceleration of soil. Accelerometer 8 to accelerometer 10 were placed on the slope to capture the acceleration of the hypotenuse part. The installation diagram of the accelerometer is shown in Fig. 5. Here, the part with accelerometers 1-7 will be called the flat part, and the part with accelerometers 8-10 will be called the slope part.

(a) Data logger

(b) Accelerometer

Fig. 4 Acceleration capture instrument in this study

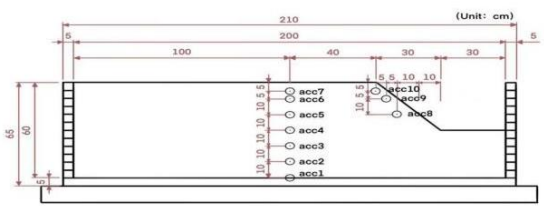

Fig. 5 Accelerometers setting in slope model

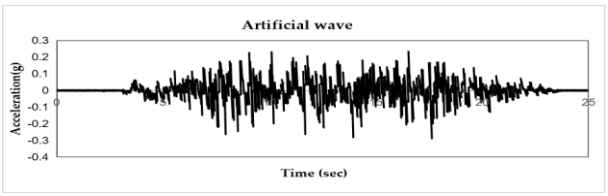

(a) Artificial earthquake wave, 0.2 g

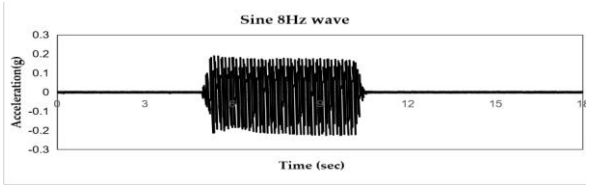

(b) Sine 8 Hz wave, 0.2 g

Fig. 6 Acceleration-time history of the input ground motions used in this study

2.3 Input motion wave

The artificial seismic wave and Sine 8Hz wave corresponding to the peak ground acceleration of 0.2 g were used to determine the basic characteristics of the slope. The artificial seismic wave used in this paper was generated according to option 1 approach 2 procedure of the US NRC the standard review plan 3.7.1 revision 4 (2014).

(1) The time history has a sufficiently small time increment (0.005s) and sufficiently long duration (more than 20 s).

(2) Spectral acceleration at 5 percent damping was computed at a minimum of 100 points per frequency decade, uniformly spaced over the log frequency scale from 0.1 Hz to 50 Hz.

(3) The computed 5 percent damped response spectrum of the acceleration time history do not fall more than 10 percent below the target response spectrum at any on frequency.

(4) The computed 5 percent damped response spectrum of the acceleration time history do not exceed the target response spectrum at any frequency by more than 30 percent (a factor of 1.3) in the frequency range of interest.

The artificial seismic wave is the synthetic seismic wave combining the Gyeongju–Pohang earthquake, using the empirical Green's function on the basis of the raw data measured in the Kori Nuclear Power Plant. As the artificial seismic wave has different periodic components, high amplification occurs. This is why the artificial seismic wave was selected to evaluate the effects of boundary conditions in the case of high amplification. The artificial seismic wave in the study is a long-period wave. Sine 8 Hz wave is a simple short-period wave that does not allow resonance to occur. The input seismic waves in this study are shown in Fig. 6.

2.4 Testing method

In this paper, 1 g shaking table test was used to obtain dynamic behavior. First, put soil samples into the soil box and compact them to a five centimeters thick layer each layer. This is to distribute the soil as evenly as possible throughout the box. Then set the accelerometer between the layers, and finally gently dig out the excess soil in the flat model to form the slope. Following this, apply the seismic

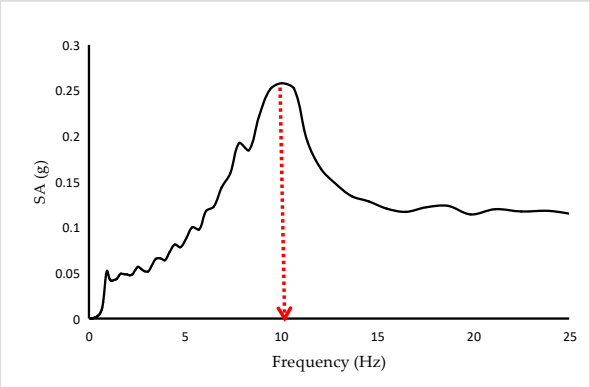

Fig. 7 The value of the natural frequency of the full tank

wave to carry out the 1 g shaking table test. Use the accelerometers and the data logger to get the experimental results.

In addition, it should be noted that before the 1 g shaking test, in order to prevent the input wave from resonating with the natural frequency of the model, a Sinesweep wave of 1-30 Hz for the full soil tank. The resonance was found to occur at 10 Hz for the full soil tank. The result is shown in Fig. 7. This was the reason why artificial seismic waves and Sine 8 Hz waves were used, based on our previous work (Kim *et al.* 2020), the natural periods of empty tank and full soil tank were 0.04-0.05 sand 0.1 s, which are very consistent with the ones observed in this study.

2.5 Numerical analysis simulation

A numerical simulation is a calculation that is run on a computer following a program that implements a mathematical model for a physical system. Numerical simulations are required to study the behavior of systems whose mathematical models are too complex to provide analytical solutions, as in most nonlinear systems. There are many numerical simulation analysis which are widely used. In this paper, 1g shaking table test and numerical analysis (ABAQUS and DEEPSOIL) were used to obtain dynamic behavior. The similar dynamic behavior of soil was verified by the two numerical analysis and the experiment.

2.5.1 ABAQUS

ABAQUS CAE is a finite element analysis and multi-physics engineering simulation software. The size models modeled by ABAQUS here are 2×0.6 m (laboratory size model), 4×1.2 m (λ=2), 10×3 m (λ=5), 20×6 m (λ=10), 40×12 m (λ=20), and the parameter used are the values in Table 3. The soil used was a homogeneous and highly compacted soil. All parameters should be calculated in proportion to Table 2 as the model size increases. The constitutive model used is the Mohr-Coulomb plastic model. The input parameters of the modeling in ABAQUS are shown in Table 5. Young's modulus is obtained by measuring the shear wave velocity. We obtained the damping ratio of the soil sample in the frequency analysis of ABAQUS. The steps are as follows:

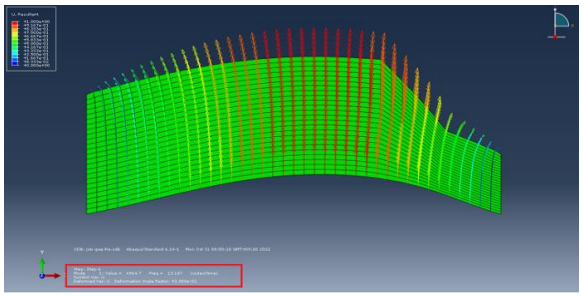

(a) The first-order natural frequency

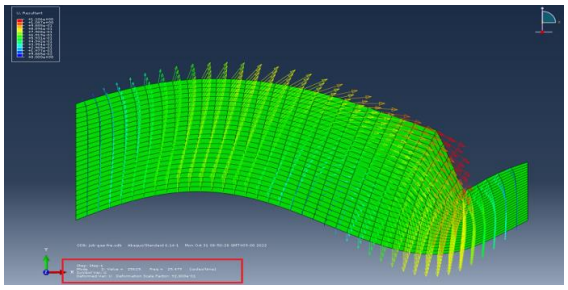

(b) The second-order natural frequency

Fig. 8 Natural frequency of the model in ABAQUS

The equation of motion can be given by Eq. (1)

$$[M_S]\{\ddot{u}_S(t)\} + \{D_S(t)\} + [K_S]\{u_S(t)\} = \{0\} \quad (1)$$

Where [Ms], [Ks], and {us(t)} are, respectively, the mass matrix, stiffness matrix, and displacement vector for a structure, and {Ds(t)} is the damping vector.

The Rayleigh damping model from Eq. (1) can be expressed by Eq. (2).

$$\{D_S(t)\} = (\alpha[M_S] + \beta[K_S])\{u_S(t)\} = \{0\} \quad (2)$$

And we obtained the circular frequency (ω1=13.187 Hz and ω2=25.779 Hz) in the frequency analysis of ABAQUS, as shown in the Fig. 8.

Coefficients α and β are given by Eqs. (3) and (4) using ($\omega 1$, $\varepsilon 1$) and ($\omega 2$, $\varepsilon 1$), Mass damping alpha removes low frequency regions α is 0.8724. Stiffness damping beta eliminates high frequency regions β is $2.566e^{-3}$.

$$\alpha = \frac{2\omega 1\omega 2\ (\delta 1\omega 2 - \delta 2\omega 1)}{\omega 2^2 - \omega 1^2} \quad (3)$$

$$\beta = \frac{2\ (\delta 2\omega 2 - \delta 1\omega 1)}{\omega 2^2 - \omega 1^2} \quad (4)$$

Where ω is the circular frequency, and h is the damping ratio.

Enter the material parameter of soil in ABAQUS as α=0.8724 and β=$2.566e^{-3.}$ The seismic input waves used in ABAQUS in this study were the artificial seismic wave and Sine 8 Hz wave.

The infinite boundary is created to eliminate the influence of the boundary on the experiment, and the boundary conditions are consistent with the laminar shear box as much as possible. The model mesh in ABAQUS is shown in Fig. 9.

Table 5 Soil input parameters used in ABAQUS

Parameter	Value	Parameter	Value
Density(kg/m^3)	1800	Young' s modulus (Pa)	2x10^7
Poisson' s ratio	0.35	Cohesion Yield Stress(kN)	10
Internal friction angle (°)	27.7	Dilatancy angle (°)	24.4
Damping (Alpha)	0.8724	Damping (Beta)	2.566e^{-3}

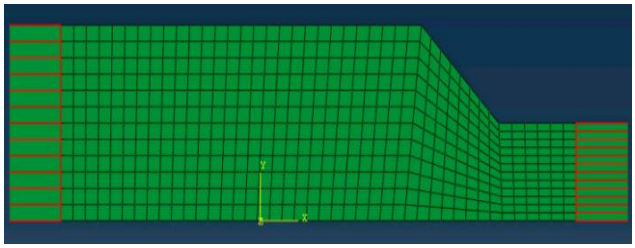

Fig. 9 Infinite boundary slope model in ABAQUS

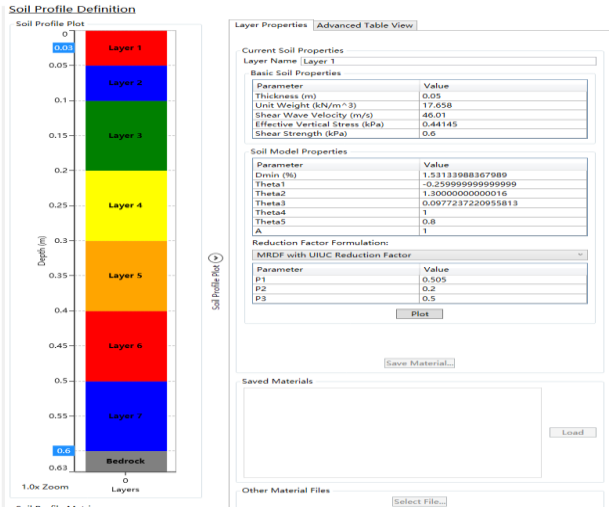

Fig. 10 1-D ground model in DEEPSOIL

Table 6 Soil input parameters used in DEEPSOIL

Parameter	Value	Parameter	Value
Thickness(m)	0.6	Unit weight(kN/m^3)	17.658
OCR	1	K_0	0.5
N	10		

2.5.2 DEEPSOIL

DEEPSOIL is a 1-D site response analysis program with graphical user-interface that can perform both: 1-D Nonlinear analysis the 1-D Equivalent linear analysis. The constitutive model used by DEEPSOIL is the Darendeli model, which is a nonlinear model. The specific parameters of the modeling in DEEPSOIL are shown in Table 6.

The model established in DEEPSOIL is shown in Fig. 10. This was designed based on the location of the accelerometers in the 1 g shaking test. Then artificial seismic wave and Sine 8 Hz wave were applied to get the analysis result. Because DEEPSOIL doesn't work well on slopes. it is used to verify the simulation results of the flat ground model.

3. Comparison and verification of simulation results and experimental results

In this study, the experimental results of 1 g shaking table test are compared with the analysis results of ABAQUS and DEEPSOIL. The modeling size of ABAQUS and DEEPSOIL are consistent with that of the 1 g shaking table. The experimental results come from the accelerometer set up in the 1 g shaking table test, and the analysis results are extracted from the accelerometer locations of the experimental setup., The Acceleration time history, 5% Damped Spectral acceleration (SA) and Spectral acceleration amplification factor (F_a) were used to compare and evaluate the experimental results and numerical analysis results, which can provide support for subsequent discussion. The dynamic behavior of soil is further studied by modeling large scale model in ABAQUS.

3.1 Comparison and verification of slope model

3.1.1 Acceleration-time history

Since the selection of all acceleration regions will provide unclear data representation, two time periods are randomly selected from artificial seismic wave and Sine 8 Hz wave to compare the Acceleration-time history. Fig. 11 shows the part of Acceleration-time history graph of 1 g shaking table test and numerical analysis for artificial seismic wave.

As for Figs. 11(a)-11(c), the experimental results of artificial seismic wave are very close to the numerical analysis results. In the flat part, the acceleration amplifies from the bottom to the top as the depth decreases. The DEEPSOIL results were slightly different from the experimental and ABAQUS results, but the change was not significant. According to Figs. 11(c) and (d), regardless of the experiment or numerical analysis, acceleration amplification of slope part is not particularly significant. The reason why the experimental results are not completely close to the numerical analysis is by using different analysis methods, DEEPSOIL uses nonlinear analysis, and ABAQUS uses iterative analysis with fixed analysis steps.

Fig. 12 shows the part of Acceleration-time history graph of 1g shaking table test and numerical analysis for Sine 8Hz wave.

In Figs. 12(a)-12(c), the experimental results of Sine 8Hz wave are very close to the numerical analysis results. In the flat part, the acceleration amplifies from the bottom to the top as the depth decreases. The experimental results are slightly different from the numerical simulation results, but not significantly According to Figs. 12(c) and 12(d), the acceleration amplification of the slope part was not particularly significant according to the numerical analysis of the experimental results of the slope part, and the acceleration part of the experimental results appeared to sink at the apex, but the numerical simulation analysis did not. This is because the acceleration was obtained by the accelerometer in the experiment, so the soil layer covering the top accelerometer is only 0.05 m. Unlike the numerical analysis, during the experiment, the friction of the soil might have caused a slight deceleration and displacement of the accelerometer. In the case of artificial seismic wave and

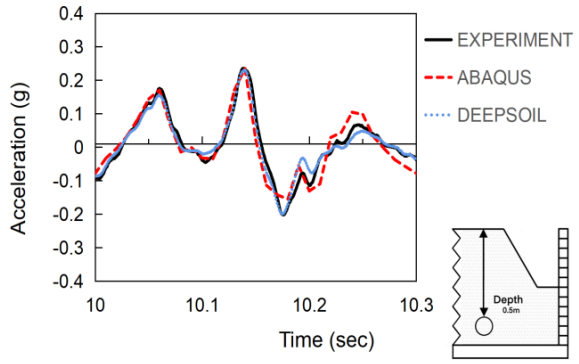

(a) Artificial seismic wave of flat part at depth 0.5 m

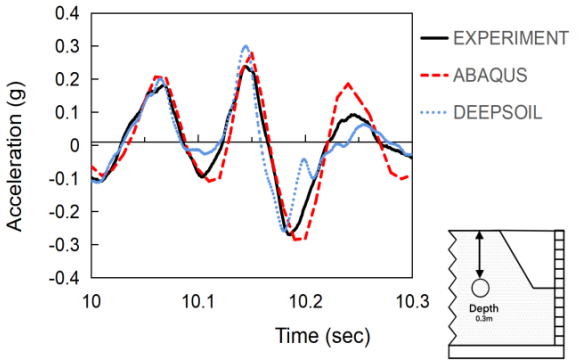

(b) Artificial seismic wave of flat part at depth 0.3 m

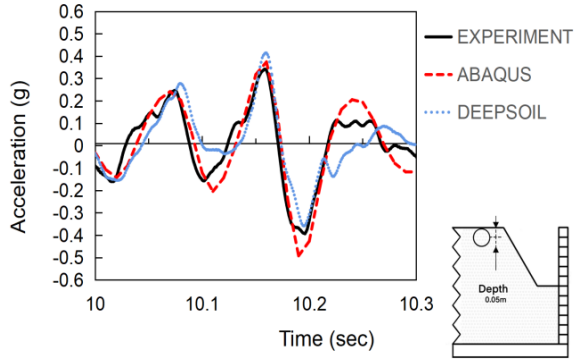

(c) Artificial seismic wave of flat part at depth 0.05 m

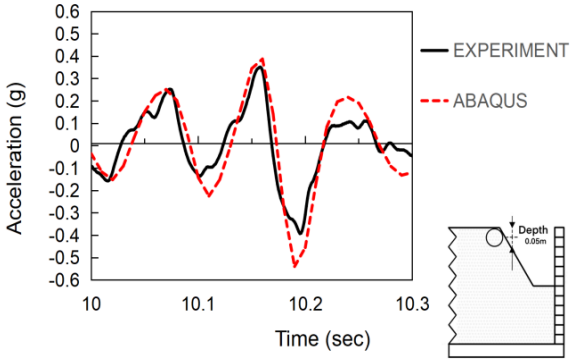

(d) Artificial seismic wave of slope part at depth 0.05 m

Fig. 11 Part of acceleration-time history graph for experiment and analysis in slope model

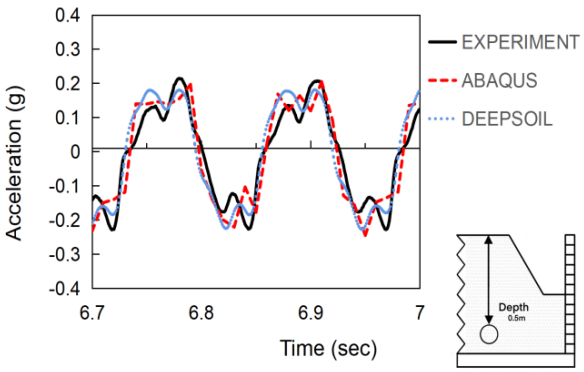

(a) Sine 8 Hz wave of flat part at depth 0.5 m

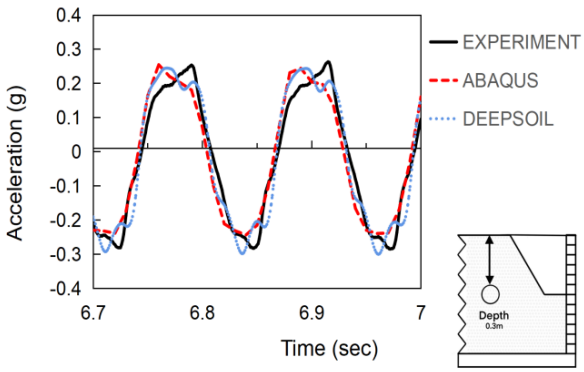

(b) Sine 8 Hz wave of flat part at depth 0.3 m

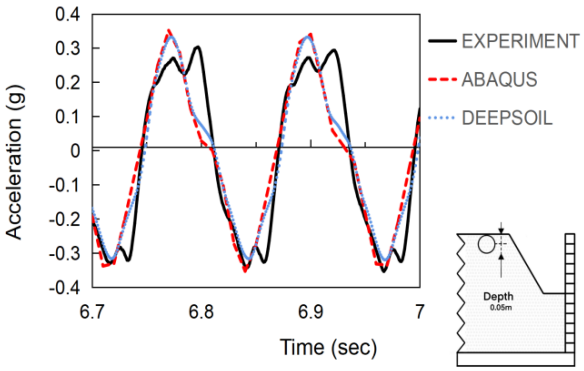

(c) Sine 8 Hz wave of flat part at depth 0.05 m

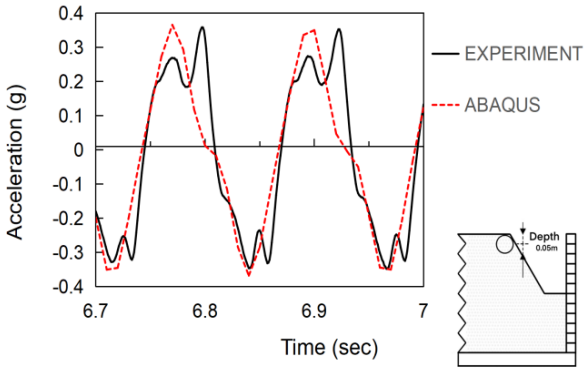

(d) Sine 8 Hz wave of slope part at depth 0.05 m

Fig. 12 Part of acceleration-time history graph for experiment and analysis in slope model

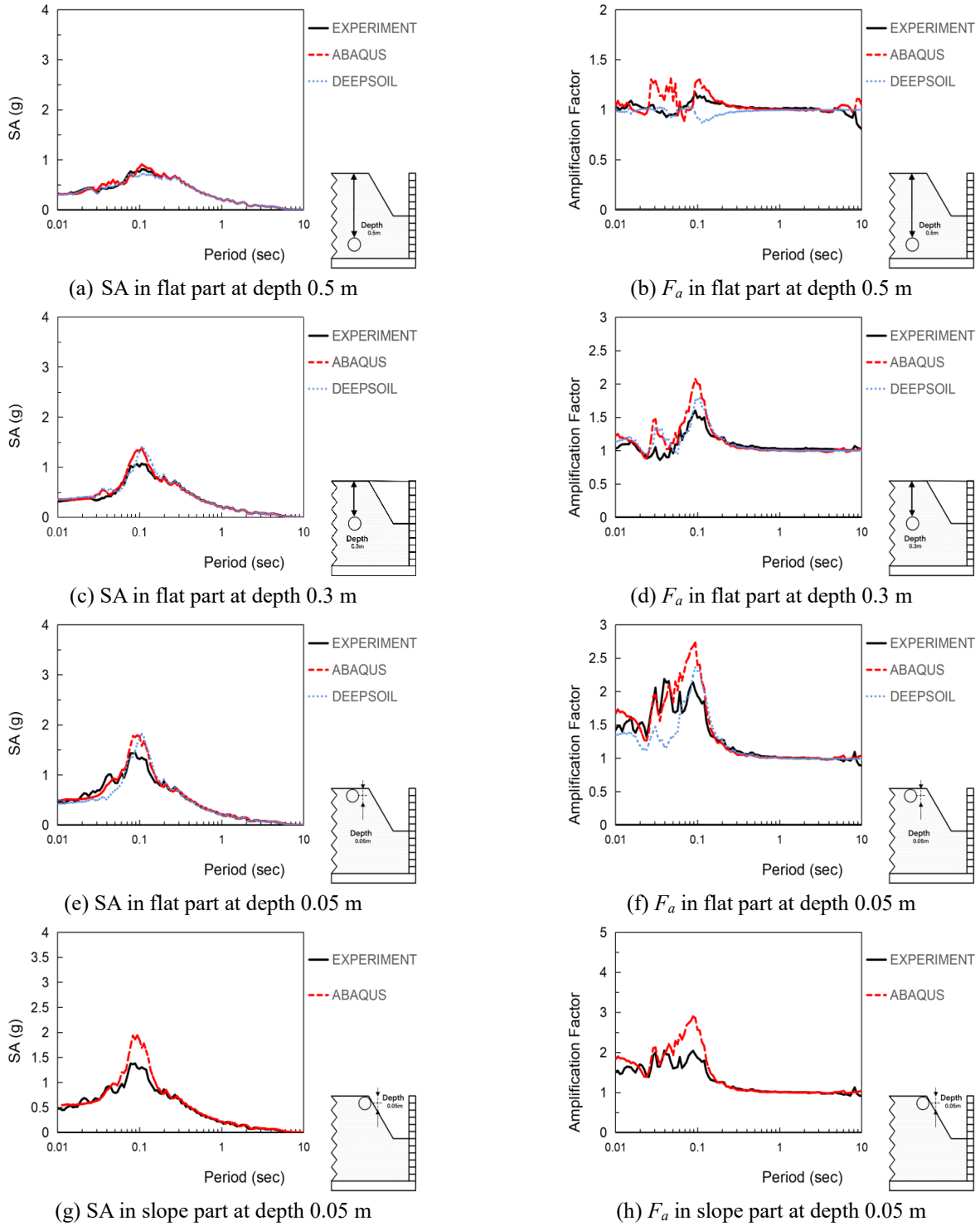

(a) SA in flat part at depth 0.5 m (b) F_a in flat part at depth 0.5 m

(c) SA in flat part at depth 0.3 m (d) F_a in flat part at depth 0.3 m

(e) SA in flat part at depth 0.05 m (f) F_a in flat part at depth 0.05 m

(g) SA in slope part at depth 0.05 m (h) F_a in slope part at depth 0.05 m

Fig. 13 Spectral acceleration and Spectral acceleration amplification factor of experiment and analysis in slope model for Artificial seismic wave

Sine 8 Hz wave, the partial accelerations of experimental and numerical results are in good agreement. Although the DEEPSOIL results are not very close, it is acceptable as an auxiliary analysis to verify the data due to the influence of boundary conditions. The experimental results are very close to the simulation results of ABAQUS, and the comparison of acceleration time history is convincing.

3.1.2 Spectral acceleration and spectral acceleration amplification factor

Spectral acceleration is the function relationship between the maximum response of a single degree of freedom elastic system to an actual seismic acceleration (acceleration, velocity and displacement) and the natural vibration characteristics of the system (natural vibration

period or frequency and damping ratio). Spectral acceleration, with a value related to the natural frequency of vibration of the building, is used in earthquake engineering (Wikipedia 2022).

For a particular soil profile and input motion, the amplification factor is computed as the ratio of Spectral acceleration at the soil surface to Spectral acceleration at the outcropping reference rock. Among many other parameters characterizing the intensity of ground motion, response spectra are generally used in engineering practice (Stambouli *et al.* 2017) because it can explain the amplifying characteristic of depth to Spectral acceleration.

Fig. 13 shows the Spectral acceleration (SA) and Spectral acceleration amplification factor (F_a) graph of 1g shaking table test and numerical analysis for artificial seismic wave

Under artificial seismic wave, it can be seen from Figs. 13(a) and 13(b) that the SA of the experimental results and numerical results are very close to each other in flat part at depth 0.5 m. In addition, Spectral acceleration amplification factor is around 1, indicating that the amplification factor between experimental results and simulation analysis is very small. From Figs. 13(c) and 13(d), the SA of numerical analysis is very close at 0.3m flat part, slightly larger than the experimental results. For the model with a natural period less than 0.1 sec, the amplification factor of numerical analysis is greater than that of experimental analysis, and for the model with a natural period greater than 0.1 sec, the amplification factor of numerical analysis is very close to that of experimental analysis. From Figs. 13(e) and 13(f), at the 0.05m flat part, when the natural period is less than 0.1 sec, the experimental analysis is close to the SA of ABAQUS. When the natural period is about 0.1 sec, the SA of ABAQUS is greater than that of the experiment. When the natural period is greater than 0.1 sec, the SA of ABAQUS is close to that of DEEPSOIL. When the natural period is about 0.1 sec, compared with the amplification factor, ABAQUS is the largest, followed by DEEPSOIL, and lastly the experiment is the lowest. From Figs. 13(g) and 13(h), the SA and amplification factor of the slope part are similar to those of the flat part at 0.05 m. In Figs. 13(a), 13(c) and 13(e), SA increases with depth. In Figs. 13(b), 13(d) and 13(f), amplification factor increases with depth.

By comparing Spectral acceleration amplification factors in flat part and slope part, ABAQUS maximizes amplification at all depths for both parts. Experimental results show that when the depth is larger, the Spectral acceleration amplification factor is greater than that of DEEPSOIL results. When the depth is small, the Spectral acceleration amplification factor of DEEPSOIL results is greater than the experimental results.

Fig. 14 shows the Spectral acceleration (SA) and Spectral acceleration amplification factor (F_a) graph of 1 g shaking table test and numerical analysis for Sine 8Hz wave.

As can be seen from Figs. 14(a) and 14(b), the SA of the experimental analysis and numerical analysis are very close to each other at the 0.5m flat part by Sine 8Hz wave, and ABAQUS results are the maximum when the natural period is less than 0.1 sec. In addition, DEEPSOIL results are the second with the smallest being the experimental results. The amplification factor is around 1 sec, indicating that the amplification factor of experimental analysis and simulation analysis is very small. From Figs. 14(c) and 14(d), the experimental analysis is very close to the SA of numerical analysis, but the SA of ABAQUS is the minimum when the natural period is 0.02 sec. When the natural period greater than 0.2 sec, the amplification factor of numerical analysis is smaller than that of experimental analysis. From Figs. 14(e) and 14(f), at the slope part of 0.05m, when the natural period is 0.01-0.02 sec, the SA of experimental analysis is greater than the numerical analysis. When the natural period is greater than 0.15 sec, the numerical analysis is smaller than the amplification factor of experimental analysis. From Figs. 14(g) and 14(h), the SA and amplification factor of experimental analysis and numerical analysis are similar to those of the flat part at 0.05m. In Figs. 14(a), 14(c) and 14(e), SA increases with depth. In Figs. 14(b), 14(d) and 14(f), amplification factor increases with depth. In general, although SA and amplification factor of experimental analysis and numerical analysis increase gradually with the decrease of depth, it is with an acceptable range.

By comparing the Spectral acceleration amplification factor, when it is less than the natural period, for flat part and slope part, with the decrease of depth, the amplification factor is the maximum in ABAQUS, and changes to the maximum in DEEPSOIL. The amplification factor gradually decreases with the increase of the natural period for flat part, and the experimental analysis value is the highest, followed by DEEPSOIL and ABAQUS. At the slope part, the experimental analysis value is larger than that of ABAQUS. One of the reasons for the difference between ABAQUS and DEPSOIL analysis may be due to the difference in constitutive models. The Mohr-Coulomb linear model was used in ABAQUS (as ABAQUS does not offer a nonlinear soil model) and the Darendeli nonlinear model was used in DEEPSOIL. However, many researchers have used these models to model the dynamic behavior of soil. In general, the experimental results are very close to the numerical results.

3.2 Large scale model analysis by ABAQUS

In this study, ABAQUS is used to model the large-scale models and analyze the dynamic characteristics. Homogeneous soil was used in the prototype, and all soil sample properties were consistent with those used in the experiment. The specific gravity of the soil was 2.69, the maximum dry unit weight was 18.27 kN/m^3, and the minimum dry weight was 12.43 kN/m^3. The optimum moisture content was 12.5% and the Atterberg limit test showed Non-Plastic (NP) for Plastic Index (PI). The maximum and minimum void ratios were 1.123 and 0.443, respectively. The fines content of the soil was 10.8% and the soil was classified as SW-SM according to the Unified Soil Classification System. The specimen was selected for the sample passing through the No. 4 sieve after the physical property tests, and the sample remaining in the No. 4 sieve was about 1% (Jin *et al.* 2021). The basis of all the models is the 1 g shaking table model mentioned above,

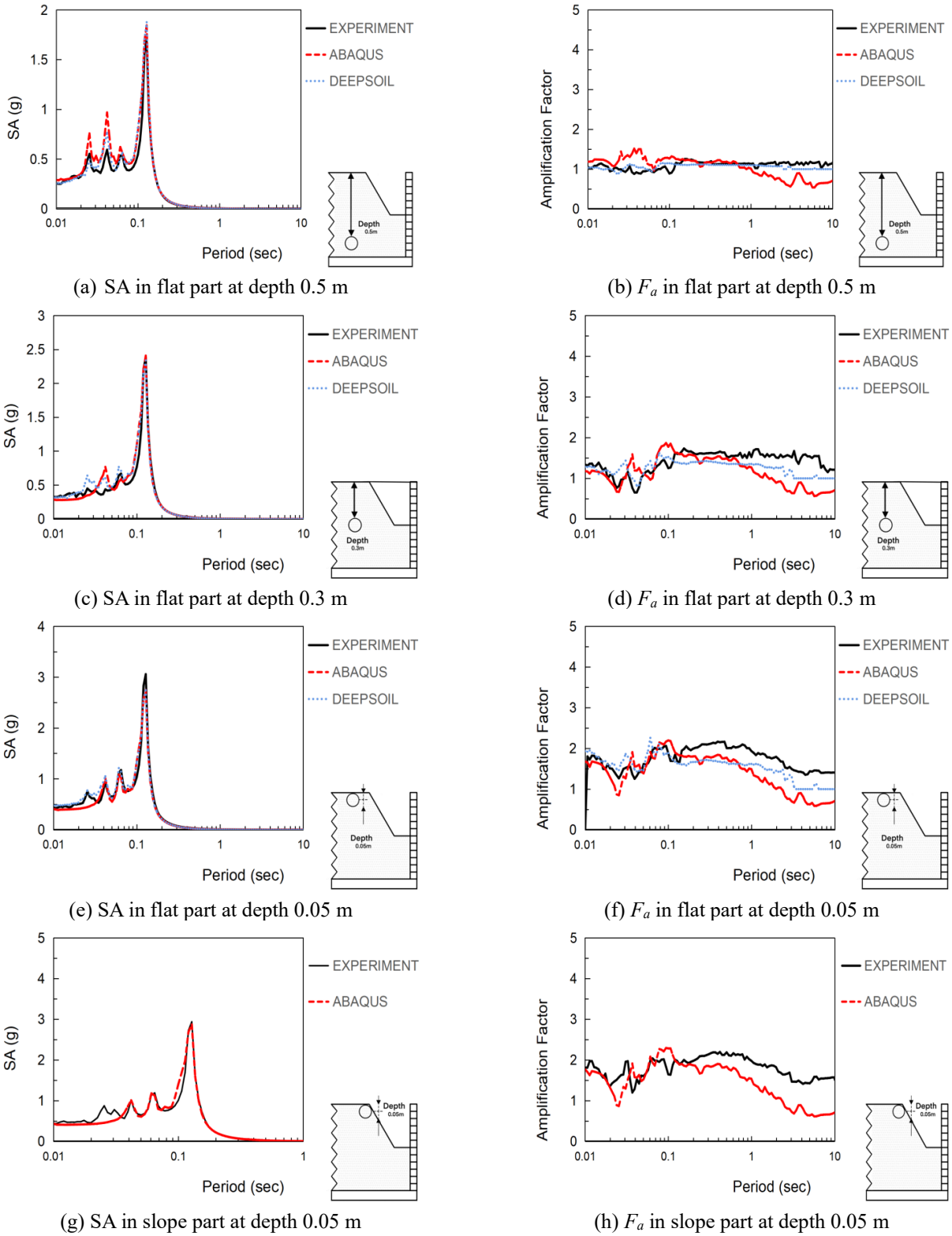

(a) SA in flat part at depth 0.5 m

(b) F_a in flat part at depth 0.5 m

(c) SA in flat part at depth 0.3 m

(d) F_a in flat part at depth 0.3 m

(e) SA in flat part at depth 0.05 m

(f) F_a in flat part at depth 0.05 m

(g) SA in slope part at depth 0.05 m

(h) F_a in slope part at depth 0.05 m

Fig. 14 Spectral acceleration and Spectral acceleration amplification factor of experiment and analysis in slope model for Sine 8 Hz wave

which is compared at the same position after magnification of 2, 4, 10 and 20 times. For example, the relationship of the similarity between the large-scale slope and 1 g shaking table model is shown in Table 7.

The numerical analysis results are shown below. Fig. 13 shows the Spectral acceleration (SA) and Spectral acceleration amplification factor (Fa) graph of numerical analysis for artificial seismic wave in different scale model.

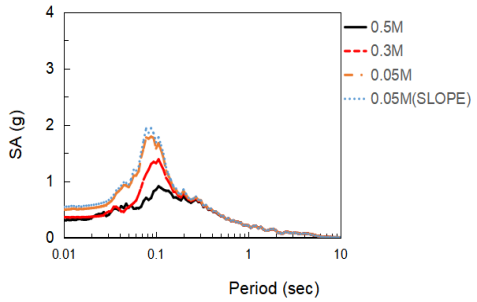

(a) SA (1 time model)

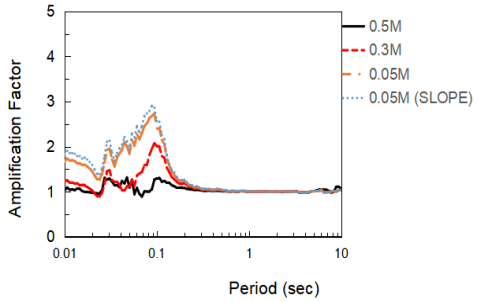

(b) Amplification factor (1 time model)

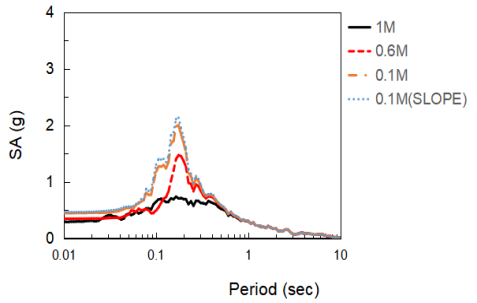

(c) SA (2 times model)

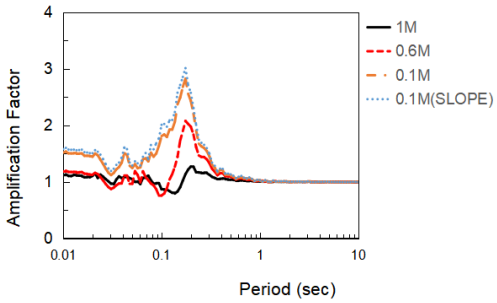

(d) Amplification factor (2 times model)

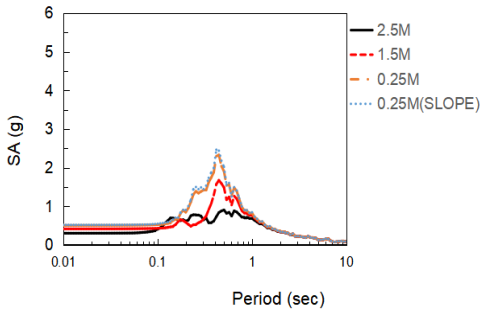

(e) SA (5 times model)

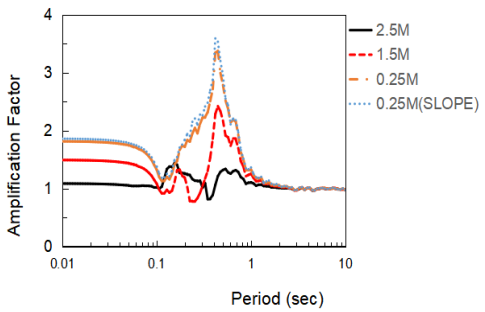

(f) Amplification factor (5 times model)

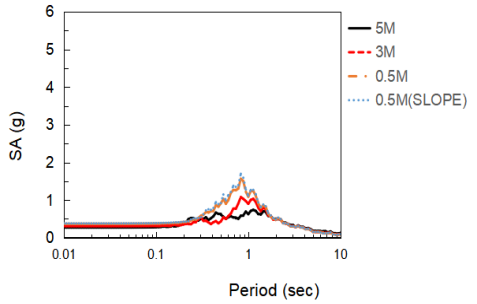

(g) SA (10 times model)

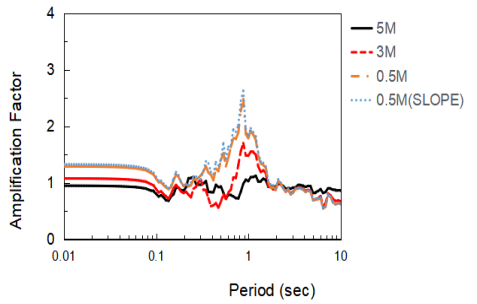

(h) Amplification factor (10 times model)

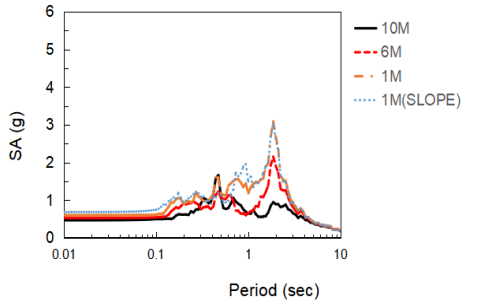

(i) SA (20 times model)

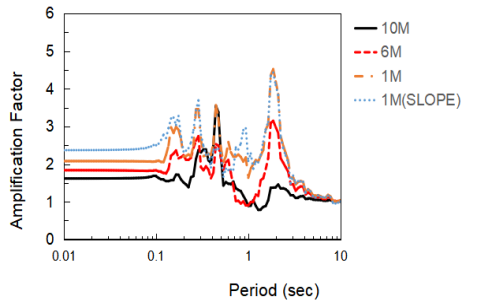

(j) Amplification factor (20 times model)

Fig. 15 Spectral acceleration and Spectral acceleration amplification factor of analysis in slope model by Artificial seismic wave in scale model

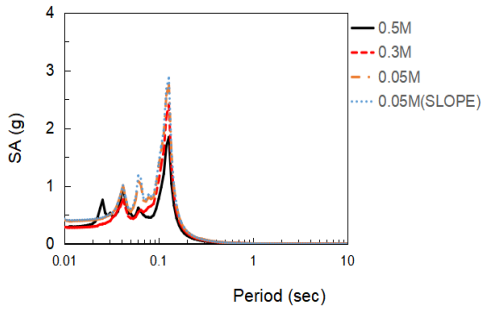

(a) SA (1 time model)

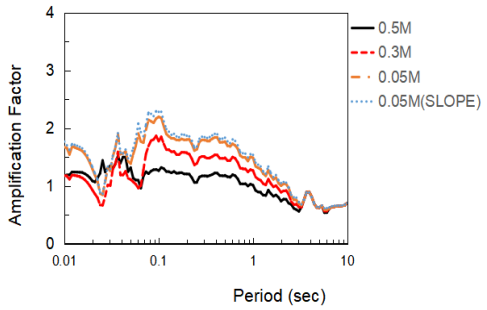

(b) Amplification factor (1 time model)

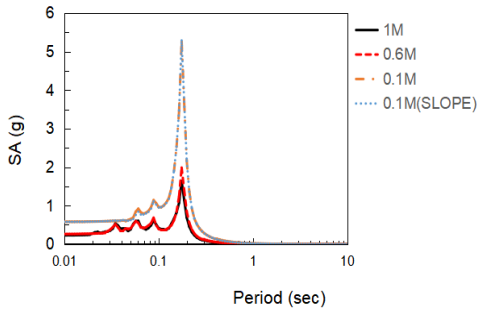

(c) SA (2 times model)

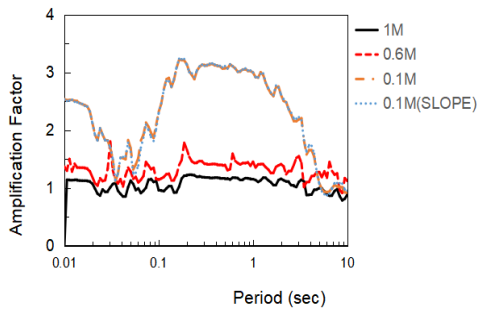

(d) Amplification factor (2 times model)

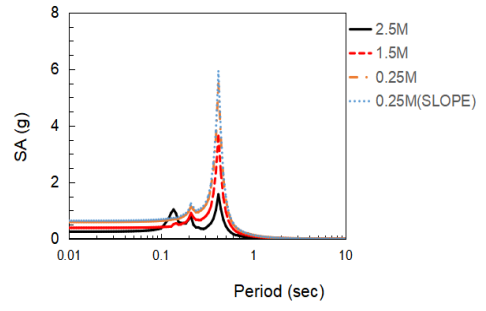

(e) SA (5 times model)

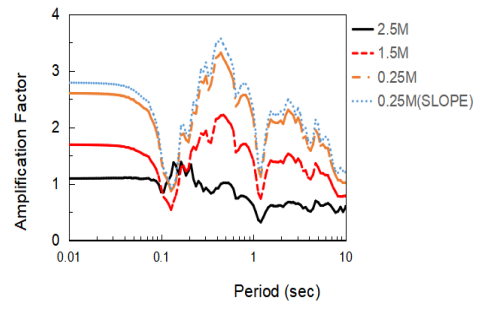

(f) Amplification factor (5 times model)

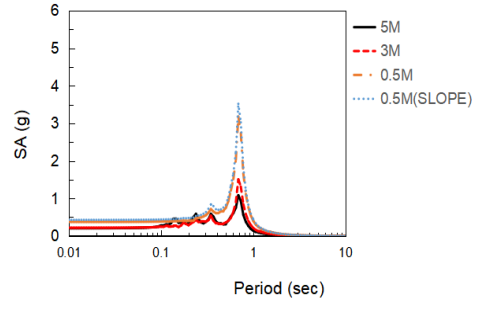

(g) SA (10 times model)

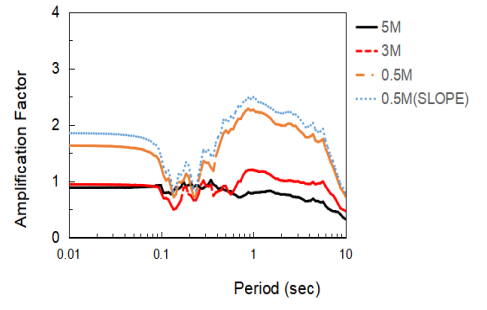

(h) Amplification factor (10 times model)

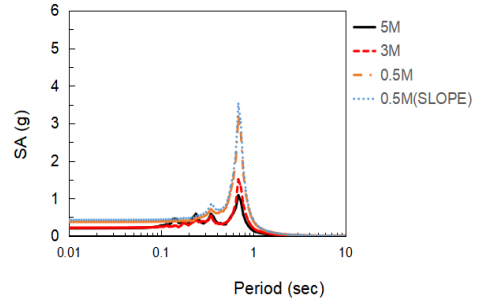

(i) SA (20 times model)

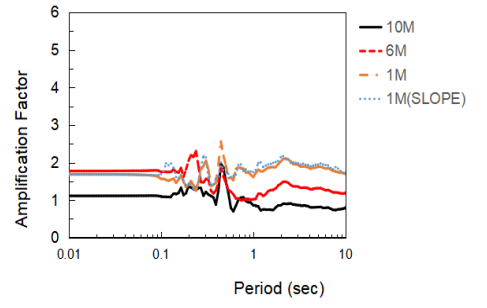

(j) Amplification factor (20 times model)

Fig. 16 Spectral acceleration and Spectral acceleration amplification factor of analysis in slope model by Sine 8 Hz wave in scale model

Table 7 Similarity relationship and scaling factors for 10 times slope model in ABAQUS

Parameter type	Model	Similarity ratio	Scaling factor	Prototype
Length	2 m	1	10	20 m
Mass density	1800 kg/m^3	1	1	1800 kg/m^3
Frequency	10 Hz	λ^{-1}	0.1	1 Hz
Modulus	2x10^7(Pa)	1	1	2x10^7(Pa)
Time	Artificial wave: 25 s Sine 8 Hz wave: 18 s	$\lambda^{0.75}$	5.623	Artificial wave: 140.585 s Sine 8Hz wave: 101.221 s
Acceleration	Artificial wave: 0.3(g) Sine 8Hz wave: 0.2(g)	1	1	Artificial wave: 0.3(g) Sine 8Hz wave: 0.2(g)

In the case of artificial seismic wave, Figs. 15(a), 15(c), 15(e), 15(g) and 15(i) show that the acceleration increases from bottom to top as the depth decreases. At the same depth, the acceleration of the slope part is greater than that of the flat part. As the size gradually increases, the frequency of the model decreases and the natural period increases, so the natural frequency at the top increases continuously from scale factor 1 to scale factor 20. Under the same natural period, as the depth decreases, the SA also increases. And at the same depth, the SA of the slope part is slightly larger than that of the flat par. From Figs. 15(b), 15(d), 15(f), 15(h) and 15(j), it can be seen that the amplification factor increases continuously from bottom to top, and the amplification factor at the slope part is greater than that at the flat part.

Fig. 16 shows the Spectral acceleration (SA) and Spectral acceleration amplification factor (F_a) graph of numerical analysis for Sine 8 Hz wave at different scale model.

In the case of Sine 8Hz wave, the Figs. 16(a), 16(c), 16(e), 16(g) and 16(i) show that the acceleration increases from bottom to top as the depth decreases. The acceleration of slope part is greater than that of flat part at the same depth. As the size gradually increases, the frequency of the model decreases and the natural period increases, so the natural frequency of the top increases continuously from scale factor of 1 to 20. Under the same natural period, as the depth decreases, the SA also increases. And at the same depth, the SA of the slope part is slightly larger than that of the flat part From Figs. 16(b), 16(d), 16(f), 16(h) and 16(j), it can be seen the amplification factor increases continuously from bottom to top, and the amplification factor at the slope part is greater than that at the flat part. Under the same conditions, similar conclusions can be obtained by using artificial seismic wave. For models with larger scales, the smaller the Spectral acceleration, the smaller amplification factor. Because of the different sizes, the natural frequencies of the model are also different,

Since the artificial seismic wave has different periodic components, the natural period of the model can be captured better by using the artificial seismic wave rather than Sine 8Hz wave. From Figs. 15(a), 15(c), 15(e), 15(g) and 15(i) under artificial seismic wave, it can be seen that the natural period is 0.1 sec when the scale factor is 1, the natural period is 0.2 sec when the scale factor is 2, the natural period is 0.5 sec when the scale factor is 5, the natural period is 1 sec when the scale factor is 10, and the natural period is 2 sec when the scale factor is 20. Based on the above data, we get the following Eq. (5)

$$\frac{\lambda}{T} = 10 \tag{5}$$

This equation can infer the natural period of the model based on the scale of the model.

And the period Eq. (6) is

$$\mathrm{T} = 2\pi\sqrt{\frac{\mathrm{m}}{\mathrm{k}}} \tag{6}$$

Where, T is the nature period. m is the mass density, and k is the stiffness coefficient.

The mass of the model is volume multiplied by density. According to the scale factor, the Eq. (7) between the nature period of the model is

$$\frac{T_p}{T_m} = \sqrt{\frac{xyz}{2\times0.6\times0.6}} = \sqrt{\frac{\lambda^3}{1^3}} \tag{7}$$

Where, T_p is natural period of the prototype. T_m is the natural period of the model. λ is the scale factor.

It should be noted here that since the model and prototype in this paper are all 2D models, the boundary of *y* (0.6 m) direction can default to infinity. So Eq. (8) can be rewritten as

$$\frac{T_p}{T_m} = \lambda \tag{8}$$

The equation for natural frequency and period is:

$$\mathrm{f} = \frac{1}{T} \tag{9}$$

Combine the Eqs. (5)- (8)- (9) and get Eq. (6)

$$\frac{\mathrm{f_p}}{\mathrm{f_m}} = \frac{1}{\lambda} \tag{10}$$

This is consistent with the similarity laws of natural frequency and size models proposed in this paper, and the accuracy of modeling using ABAQUS is verified by calculating the period and frequency of the model. Therefore, the values in the numerical model conform to the equations and scale factors. ABAQUS was used to model the large-scale model, and the feasibility was verified by a number of model results and analysis.

4. Conclusions

This study has been done to investigate the feasibility of the 1 g shaking table test for the prediction of the dynamic behavior of the real scale slope based on the 1 g shaking table test. Firstly, model ground was prepared in laminar shear box, and the experimental data were obtained for using artificial seismic wave and Sine 8 Hz wave. The results of 1g shaking table test were compared with the results of ABAQUS and DEEPSOIL. According to the results of 1 g shaking table test, the similarity law is used to analyze the large-scale model. The conclusions of this study are as follows:

• According to the experimental results and numerical analysis results, under the seismic input wave in the same size model, the acceleration from bottom to top was amplified with the decrease of depth. The acceleration of the experimental results at the surface, unlike the numerical results, seems to be unstable at the apex, which may be caused by the friction between the soil and the accelerometer. For spectral acceleration, regardless of a consistent frequency with the flat ground or slope, the experimental results and numerical analysis results are almost identical, especially at maximum amplification. By comparing the spectral acceleration amplification factors, in general, the experimental results are very close to the numerical analysis results. This indicates that there is little difference in the amplification of the respective outcropping reference rock.

• The dynamic behavior of the slope model from the numerical analysis is consistent with that from the 1g shaking table test. It is shown that the laminar shear box can minimize the influence of the boundary on the dynamic behavior of the soil. The laminar shear box is evaluated to have good performance for slope model. Numerical analysis of slope model using ABAQUS and DEEPSOIL is pretty closed. The results of ABAQUS analysis were in good agreement with those of the experimental analysis. However, due to the different constitutive models, some of the results were also different, but this was within the acceptable range.

• In the model of the same size, regardless of flat ground or slope, the spectral acceleration increases with the decrease of depth. With the increase of modeling size, the maximum spectral acceleration also changes with the change of model frequency. The spectral acceleration amplification factor is also related to the frequency of the model. The maximum amplification factor is found at the natural frequency of the model, and the maximum amplification factor increases with the decrease of the depth, which is basically the same regardless of flat ground or slope.

• In the process of modeling according to the similarity law with ABAQUS, with the increase of ABAQUS modeling size, the frequency decreases with the size. The maximum natural period also increases with the size, and there is a proportionality constant between the scale factor and natural period. It is consistent with the law of similitude for frequency and scale models, confirming the positive evaluation of model modeling using ABAQUS.

• It is very difficult to simulate a real scale slope ground using 1g shaking table test. The dynamic behavior of scale-down slope under seismic input waves can be obtained through the 1g shaking table test, and the real scale slope ground can be studied by using the numerical analysis through the similarity law. Combined with the natural frequency of the real slope, the similarity law is compared with the slope model of 1g shaking table test, and the results are in good agreement. It shows that based on the 1g shaking table test, the research on the size model is feasible, and the dynamic characteristics of the real slope can be predicted.

• In this study, an extensive numerical analysis has been performed to overcome the size limitation of 1g shaking table test in predicting the dynamic behavior of real scale slope. In this study, an extensive numerical analysis has been performed to overcome the size limitation of 1g shaking table test in predicting the dynamic behavior of real scale slope. An equation has been developed to obtain natural frequency of the real scale model. In actual earthquake engineering, the natural frequency can be obtained by this method. The prediction and analysis of the dynamic characteristics of large-scale models by numerical analyses along with the 1g shaking table test is very meaningful, and this will become one of the main research directions in the future.

Acknowledgments

The research described in this paper was financially supported by Chosun University (2021).

References

Chen, S., Zhuang, H., Quan, D., Yuan, J., Zhao, K. and Ruan, B. (2019), "Shaking table test on the seismic response of large-scale subway station in a loess site: A case study", *Soil. Dyn. Earthq. Eng.*, **123**, 173-184. https://doi.org/10.1016/j.soildyn.2019.04.023.

Corominas, J., van Westen, C., Frattini, P., Cascini, L., Malet, J.P., Fotopoulou, S., Catani, F., van den Eeckhaut, M., Mavrouli, O., Agliardi, F., Pitilakis, K., Winter, M.G., Pastor, M., Ferlisi, S., Tofani, V., Hervás, J. and Smith, J.T. (2014), "Recommendations for the quantitative analysis of landslide risk", *Bull. Eng. Geol. Environ.*, **73**(2), 209-263. https://doi.org/10.1007/s10064-013-0538-8.

Coutinho, C.P., Baptista, A.J. and Rodrigues, J.D. (2016), "Reduced scale models based on similitude theory: a review up to 2015", *Eng. Struct.*, **119**, 81-94. https://doi.org/10.1016/j.engstruct.2016.04.016.

Darendeli, M.B. (2001), "Development of a new family of normalized modulus reduction and material damping curves", PhD. dissertation,The university of Texas, Austin.

Iai, S. (1989), "Similitude for shaking table tests on soil-structure-fluid model in 1g gravitational field", *Soils Found.*, **29**(1), 105-118. https://doi.org/10.3208/sandf1972.29.105.

Jin, Y., Kim, H., Kim, D., Lee, Y. and Kim, H. (2021), "Seismic Response of Flat Ground and Slope Models through 1 g Shaking Table Tests and Numerical Analysis", *Appl. Sci.*, **11**(4), 1875. https://doi.org/10.3390/app11041875.

Kawaga, T. (1978), "On the similitude in model vibration tests of earth-structures", *J. Jpn. Soc. Civ. Eng.*, **1978**(275), 69-77. https://doi.org/10.2208/jscej1969.1978.275_69.

Keefer, D.K. (1984), "Landslides caused by earthquakes", *Geol. Soc. Am. Bull.*, **95**(4), 406-421. https://pubs.er.usgs.gov/publication/70014049.

Kim, H., Jin, Y., Lee, Y., Kim, H. S. and Kim, D. (2020), "Dynamic Response Characteristics of Embankment Model for Various Slope Angles", *J. Korean. Phys. Soc.*, 19(2), 35-46. https://doi.org/10.12814/jkgss.2020.19.2.035.

Kim, H., Kim, D., Lee, Y. and Kim, H. (2020), "Effect of soil box boundary conditions on dynamic behavior of model soil in 1 g shaking table test", *Appl. Sci.*, **10**(13), 4642. https://doi.org/10.3390/app10134642.

Liao, H.W. and Lee, C.T. (2000), "Landslides triggered by the Chi-Chi earthquake", *In Proceedings of the 21st Asian conference on remote sensing*, Taipei.

Lin, M.L. and Wang, K.L. (2006), "Seismic slope behavior in a large-scale shaking table model test", *Eng. Geol.*, **86**(2-3), 118-133. https://doi.org/10.1016/j.enggeo.2006.02.011.

Meymand, P.J. (1998), "Shaking table scale model tests of nonlinear soil-pile-superstructure interaction in soft clay", PhD. dissertation, University of California, Berkeley.

Moghadam, M.R. and Baziar, M.H. (2016), "Seismic ground motion amplification pattern induced by a subway tunnel: shaking table testing and numerical simulation", *Soil. Dyn. Earthq. Eng.*, **83**, 81-97. https://doi.org/10.1016/j.soildyn.2016.01.002.

Rocha, M. (1957), "The possibility of solving soil mechanics problems by the use of models", *Proceedings of the 4th Int. Conf. on SMFE*.

Roscoe, K.H. (1968), "Soils and model tests", *J. Strain. Anal. Eng.*, **3**(1), 57-64. https://doi.org/10.1243/03093247V031057.

Seo, S., Lim, H. and Chung, M. (2021), "Evaluation of failure mode of tunnel-type anchorage for a suspension bridge via scaled model tests and image processing", *Geomech. Eng.*, **24**(5), 457-470. https://doi.org/10.12989/gae.2021.24.5.457.

Stambouli, A.B., Zendagui, D., Bard, P.Y. and Derras, B. (2017), "Deriving amplification factors from simple site parameters using generalized regression neural networks: implications for relevant site proxies", *Earth. Planets. Space.*, **69**(1), 1-26. https://doi.org/10.1186/s40623-017-0686-3.

Sukkarak, R., Pramthawee, P., Jongpradist, P., Kongkitkul, W. and Jamsawang, P. (2018), "Deformation analysis of high CFRD considering the scaling effects", *Geomech. Eng.*, **14**(3), 211-224. https://doi.org/10.12989/gae.2018.14.3.211.

Tian, Y., Owen, L.A., Xu, C., Shen, L., Zhou, Q. and Figueiredo, P.M. (2020), "Geomorphometry and statistical analyses of landslides triggered by the 2015 Mw 7.8 Gorkha Earthquake and the Mw 7.3 Aftershock, Nepal", *Front. Earth Sci.*, **8**, 407. https://doi.org/10.3389/feart.2020.572449.

Turan, A., Hinchberger, S.D. and El Naggar, H. (2009), "Design and commissioning of a laminar soil container for use on small shaking tables", *Soil. Dyn. Earthq. Eng.*, **29**(2), 404-414. https://doi.org/10.1016/j.soildyn.2008.04.003.

Wikipedia (2022), https://en.wikipedia.org/wiki/Spectral_acceleration.

Xu, C., Xu, X., Yao, X. and Dai, F. (2014), "Three (nearly) complete inventories of landslides triggered by the May 12, 2008, Wenchuan Mw 7.9 earthquake of China and their spatial distribution statistical analysis", *Landslides.*, **11**(3), 441-461. https://doi.org/10.1007/s10346-013-0404-6.

Yang, G., Qi, S., Wu, F. and Zhan, Z. (2018), "Seismic amplification of the anti-dip rock slope and deformation characteristics: A large-scale shaking table test", *Soil Dyn. Earthq.Eng.*, **115**, 907-916. https://doi.org/10.1016/j.soildyn.2017.09.010.